Study on thermal conductivities of Si thin films and porous Si structures based on a modified lattice Boltzmann method

Ping Zhou, Lei Ma, Wei Liu, and Zhichun Liu

Citation: Journal of Applied Physics **124**, 104302 (2018); doi: 10.1063/1.5040127
View online: https://doi.org/10.1063/1.5040127
View Table of Contents: http://aip.scitation.org/toc/jap/124/10
Published by the American Institute of Physics

Study on thermal conductivities of Si thin films and porous Si structures based on a modified lattice Boltzmann method

Ping Zhou,[1] Lei Ma,[2] Wei Liu,[1] and Zhichun Liu[1,a)]
[1]*School of Energy and Power Engineering, Huazhong University of Science and Technology, Wuhan 430074, China*
[2]*School of New Materials and New Energies, Shenzhen Technology University, Shenzhen 518118, People's Republic of China*

(Received 14 May 2018; accepted 24 August 2018; published online 12 September 2018)

In this work, a modified lattice Boltzmann method (LBM) is developed to predict the thermal conductivity of silicon thin films and porous silicon structures, in which a probability parameter is introduced to determine whether a phonon collision event happens at a specific lattice point. The thickness dependent silicon thin film thermal conductivity calculated using this method shows a good agreement with prior experimental and simulation results. We also use this approach to study the porosity and pore-size dependent thermal conductivity of porous silicon structures. Furthermore, the simulated results about thermal conductivity of porous silicon are found to agree well with the previously reported data. The modified algorithm offers substantial computational improvement as compared to current LBM models and enables us to a clearer understanding about the meaning of collision step and streaming step in the LBM model. *Published by AIP Publishing.*
https://doi.org/10.1063/1.5040127

I. INTRODUCTION

The rapid advancement of microelectronics and optoelectronics systems has caused monocrystalline silicon thin films to become increasingly popular in engineering applications. A comprehensive understanding of the thermal properties of silicon thin films is urgently required because significantly high heat flow will influence device performance and reliability.[1,2] However, predicting the thermal properties of thin films is difficult owing to the breakdown of the Fourier heat diffusion theory at length scales comparable to the heat carriers' mean free paths (MFPs).[3,4] Moreover, by adjusting the porosity and pore size of the porous silicon, the thermal conductivity is found to be two or three orders of magnitude lower than the silicon bulk value. These porous silicon structures have uses as thermal insulators in microsensors and microsystems and have been of research interest for a long time.[5–7]

The lattice Boltzmann method (LBM) is a particle-based method that uses the finite differencing approach to numerically solve the phonon Boltzmann transport equation (BTE). The LBM simulates the evolution of the directional and spatial distribution of particles in the phase space.[8] Both gray and frequency dependent LBM models have been developed. The former model treats the material using a single phonon relaxation time and MFP, while the latter explicitly incorporates the phonon dispersion in the calculation. Utilizing the gray model, Sellan *et al.* computed the cross-plane lattice thermal conductivity of silicon thin films down to 17.4 nm.[9] Escobar and Amon studied phonon transport across thin films based on the dispersion LBM model and found that the film thermal conductivity decreased much faster than the solution of the gray LBM model predicted.[10] A few other studies that made use of the LBM model to examine the thermal transport in applications range from electronic cooling to data storage.[11,12] Under the framework of the LBM model, Heino recently investigated the impact of optical phonons on the thermal transport around a nanoscale hot spot.[13] He observed a temperature slip across the spot-medium boundary and the dependence of the thermal boundary resistance at the spot-medium interface on the optical phonon relaxation rate. Christensen *et al.* coupled the LBM model with the finite difference method to analyze the heat transport in a 2D domain and obtained a good agreement with the experimental results.[14] On studying the thermal transport in 2D structures, Nabovati *et al.* found that in transient ballistic phonon heat conduction, the D2Q7 lattice yields a superior performance than the D2Q9 lattice.[8] Jiang and Ho proposed an LBM that took into account the phonon dispersion and interaction between phonons of different polarizations to study phonon hydrodynamics.[15] Typically, the LBM model is also used to study the thermal transport in the high Knudsen number regime. (Knudsen number is defined as the ratio of the phonon MFP to the characteristic device length scale.)

Although the LBM model has comprehensively applied in the phonon transport simulation area, some problems cannot avoid when this method is selected for computation. First, some input parameters, such as bulk phonon properties (frequency and group velocity), should be accuracy computed before simulation, which means that the LBM should combined with other method, such as lattice dynamics,[9,16] when it is applied in a specific solid heat transfer problems. Second, large amount of calculation is also a trouble when we use LBM to simulate a complicated structure, although it has an advantage for its simply boundary treatment, especially for a 3D simulation. Third, the gray LBM and the

a)Author to whom correspondence should be addressed: zcliu@hust.edu.cn

dispersion LBM are two main models for phonon transport simulation, which has been mentioned before, and both methods have their pros and cons. For the gray LBM model, it considers a liner dispersion relation, in which only a single, frequency independent phonon mode is included. So the gray LBM model is simply a small amount of calculation. But obviously, this simplified method is lack of accuracy compared to the dispersion model, which considers the non-liner dispersion in order to accurately predict the phonon transport. So it is hard to balance the accuracy and the computational efficiency.

In this work, we develop a modified LBM model which introduces a probability parameter P to determine whether phonon scattering occurs at a given lattice point. The introduction of the probability parameter is analogous to the treatment of phonon scattering in the stochastic Monte Carlo simulation of thermal transport.[17] During the simulation, at each time step, a random number generates at every lattice point, and these random numbers are compared with P to determine whether the scattering will take place in the lattice site. A phonon collision happens at a lattice point when the drawn random number is greater than the probability P. We used this newly proposed transport model to simulate phonon transport in silicon thin films and porous silicon structures. The main objective of present paper is to propose a modified LBM to calculate the nanoscale thermal conductivity. Compared with current LBM, this modified LBM can greatly save computing time, and its verification is conducted by comparing the calculation results with the prior experimental data for both thin films and porous structures.

II. SIMULATION METHODOLOGY

Phonon transport generally consists of cumulative contributions of all the phonon modes and this transport mechanism is governed by the BTE. The phonon BTE is an integro-differential equation that tracks the evolution of the phonon distribution function in the 6D-phase space and is generally difficult to solve. To make the simulations tractable, we use the LBM, a discrete expression of the BTE, to model the size-dependent thermal transport in thin films and porous structures.

Neglecting the external force term, the transient phonon BTE under the single mode relaxation time approximation can be written as[18]

$$\frac{\partial f}{\partial t} + \vec{v}_g \cdot \nabla f = \frac{f^{eq} - f}{\tau}, \tag{1}$$

where t is the simulation time, and f, $\vec{v}_g$, and τ are the phonon number distribution function, phonon group velocity, and phonon lifetime of the material under study, respectively. The term f^{eq} in Eq. (1) is the phonon equilibrium distribution function and is described by the Bose–Einstein distribution

$$f^{eq} = \frac{1}{e^{\hbar\omega/\mathrm{k}_B T} - 1}, \tag{2}$$

where $\hbar\omega$ is the phonon quanta energy, k_B is the Boltzmann constant, and T is the equivalent equilibrium lattice temperature. If assuming gray phonon properties in the first-order discretization of the phonon BTE in time and space, we obtain the discrete lattice Boltzmann equation[19]

$$f_\alpha(x + \Delta x, t + \Delta t) - f_\alpha(x, t) = \frac{\Delta t}{\tau}\left[f_\alpha^{eq}(x, t) - f_\alpha(x, t)\right], \tag{3}$$

where x is the spatial coordinate, the subscript α represents the discretized phonon propagation directions at each lattice site, f_α and f_α^{eq} are the corresponding directional phonon distribution function and equilibrium distribution function, respectively, and Δt is the computational time step related to the lattice spacing $\Delta \mathrm{x} = \mathrm{v}_{\mathrm{g},\alpha} \times \Delta \mathrm{t}$, where $v_{g,\alpha}$ is the group velocity along the direction α.

In the LBM model, a lattice type is typically described as "DnQm" in which "n" represents the dimension and "m" stands for the discrete number. For 2D simulations, the D2Q7 lattice and the D2Q9 lattice are commonly used. Compared with the latter, the D2Q7 lattice provides more accurate simulation results. However, the D2Q9 lattice is preferred in most studies owing to its simple structure and more straightforward boundary condition (BC) implementation.

In this work, we use the D2Q9 lattice in the LBM simulations. As shown in Fig. 1, at each lattice point, there are eight different velocities that can be expressed as follows:

$$e_\alpha = \begin{cases} (0,0), & \alpha = 0 \\ \left(\cos\left[(\alpha-1)\pi/2\right], \sin\left[(\alpha-1)\pi/2\right]\right)c, & \alpha = 1,2,3,4 \\ \left(\cos\left[(2\alpha-1)\pi/4\right], \sin\left[(2\alpha-1)\pi/4\right]\right)\sqrt{2}c, & \alpha = 5,6,7,8, \end{cases} \tag{4}$$

where c is the phonon group velocity in the materials being examined.

In the current LBM simulation, one time step includes two processes. For the first process, the distribution functions at one lattice site move in the direction of the assigned discrete velocity towards the next lattice site, so this process is called streaming step. For the second process, phonons that come from different directions gather in one lattice site and collide with each other, and based on the specified collision rules, new distribution functions are calculated at each lattice site for the next time step, so this process is called collision step. The phonons follow similar recurring events at every time step until the attainment of equilibrium. Because distribution functions at each lattice site are determined by the surrounding lattice points, the effect of the BCs is also included in the computation for the new components of the

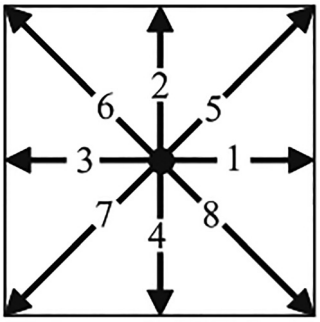

FIG. 1. D2Q9 lattice.

distribution functions at each lattice site. More details can be seen in the introduction of BC.

In this study, we propose a new collision rule to model the phonon scattering under the framework of the LBM model. Similar to the treatment of phonon scattering in the Monte Carlo simulations, we introduce a probability parameter P to determine the occurrence of collision events. As discussed in Ref. 16, the phonon scattering probability is given by

$$P = 1 - \exp(-\Delta t/\tau). \tag{5}$$

To determine whether a scattering event occurs, a random number is generated at every lattice point and compared with P. If the random number is greater than P, a collision occurs and the evolution of the distribution function is given by

$$f_\alpha(x + \Delta x, t + \Delta t) = f_\alpha^{eq}(x, t). \tag{6}$$

However, if the random number is less than P, no scattering occurs and the phonons only travel through the lattice. In this case, the evolution of the distribution function is described by

$$f_\alpha(x + \Delta x, t + \Delta t) = f_\alpha(x, t). \tag{7}$$

In the Monte Carlo method, this probability P is for a phonon bundle to be scattered (internal scattering). For example, if the phonon bundle is scattered, the states of the phonon bundle will be reset (include frequency, branch, velocity, and direction). So in our LBM model, we think in the gray model, the states of phonon bundle are some statistical average values except for direction, so in the stream-collision step, if the phonon bundle is scattered, the collision step will take place, the numbers of phonons in different directions will reset according to the collision rule. Based on this, we conjecture that the phonon bundle scatter probability is just the collision step probability, and the simulation results show that our guess is true.

After updating the new components of the local distribution functions at the end of each time step, the total distribution function and the heat flux can be computed as follows:

$$f(x, t) = \sum_{\alpha=0}^{8} f_\alpha(x, t), \tag{8}$$

$$q_n(x, t) = \left[\sum \left(f_{in}(x, t)\cos\theta - f_{out}(x, t)\cos\theta\right)\right] \times \hbar\omega v_g D_\omega \Delta\omega d/\pi, \tag{9}$$

where n represents the heat flux direction, θ is the angle between the phonon propagation direction and the flux direction n, D_ω is the phonon density of states, $\Delta\omega$ is the frequency bandwidth (equal to ω for the gray model), and d is the dimension of space. The average phonon frequency is

$$\omega = \frac{k_B T_D}{\hbar}, \tag{10}$$

where T_D is the material Debye temperature, and $\hbar$ is the Planck constant divided by 2π. The density of states can be calculated from

$$D_\omega = \frac{c_v}{k_b(\hbar\omega/k_bT)^2 e^{(\hbar\omega/k_bT)}\left(e^{(\hbar\omega/k_bT)} - 1\right)^{-2}\Delta\omega}. \tag{11}$$

The local temperature at each lattice site can be computed by inverting Eq. (2) as follows:[20]

$$T(x, t) = \frac{\hbar\omega}{k_B \log\left(\frac{1}{f^{eq}(x, t)} + 1\right)}. \tag{12}$$

It is important to implement the correct BCs in the LBM model. In this work, we mainly use the periodic BC and bounce back BC. Periodic BC means that the phonons leaving one side of the computational domain will enter the domain from another corresponding boundary without any property change. This type of BC is typically used when dealing with periodic structures with infinite domains. For the left and right boundaries shown in Fig. 2(a), we apply the periodic BC to obtain

$$f_{1,5,8}(0, j) = f_{1,5,8}(NX, j) \text{ and } f_{3,6,7}(NX, j) = f_{3,6,7}(0, j).$$

For the bounce back BC, the particle is assumed to simply reverse its travelling direction after colliding with a boundary, as shown in Fig. 2(b). Therefore, we obtain

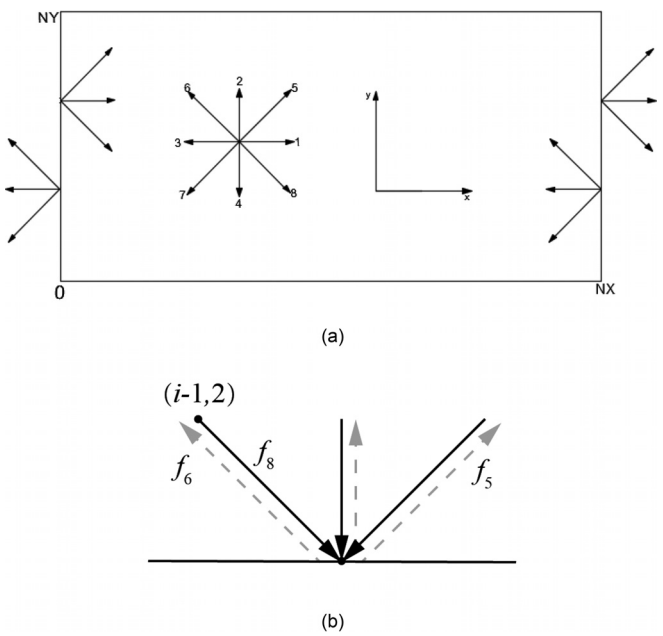

FIG. 2. BCs for the D2Q9 lattice. (a) Periodic BC. (b) Specular reflection BC.

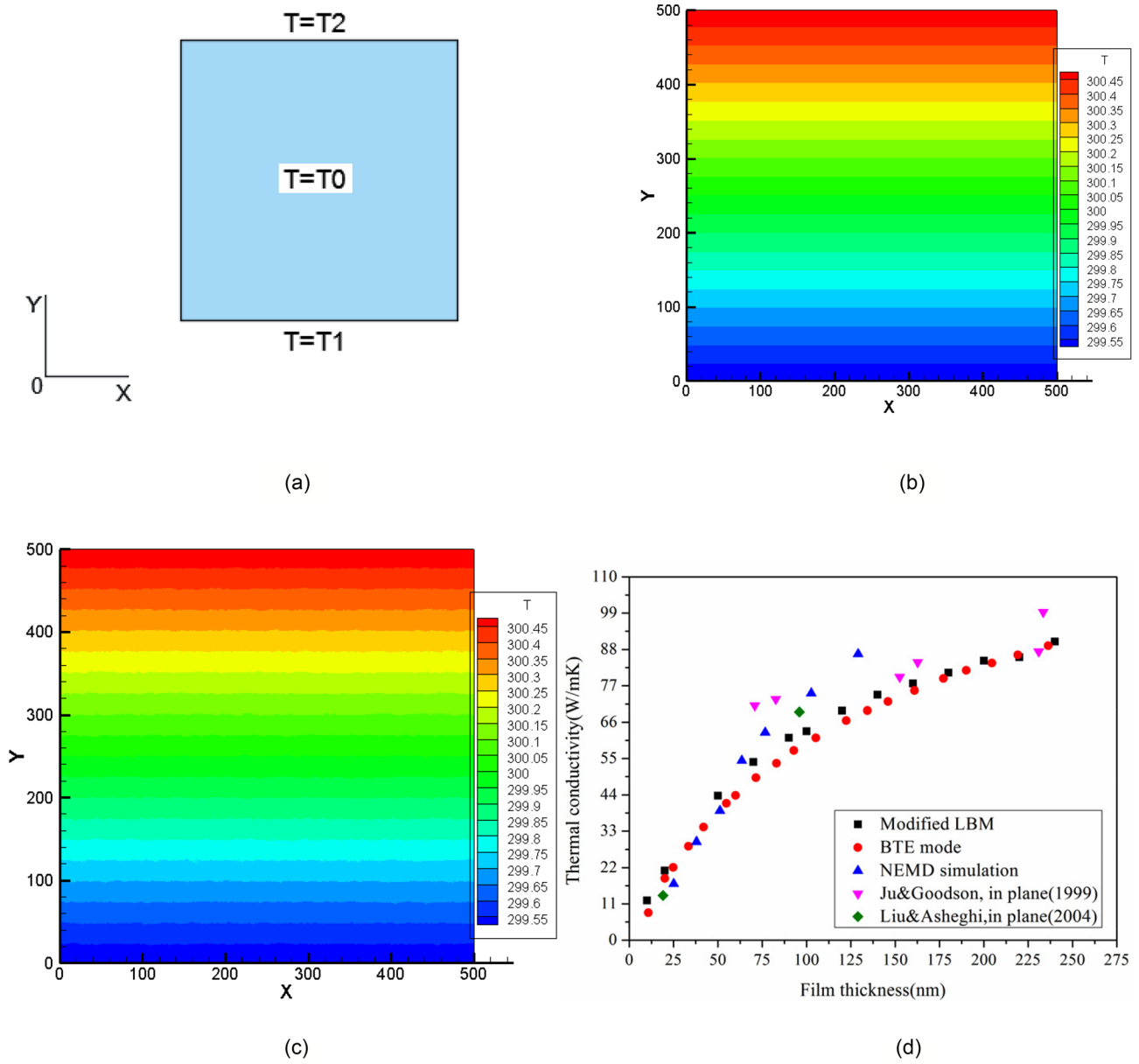

FIG. 3. D2Q9 lattice used in simulation of temperature distribution and conductivity in the silicon film. (a) Silicon thin film subject to constant temperature BCs. (b) Temperature distribution inside the silicon thin film predicted by the current LBM model. (c) Temperature distribution inside the silicon thin film predicted by the modified LBM model. (d) Thickness-dependent thermal conductivity of silicon thin film.

$f_{2,5,6}(i,1) = f_{4,7,8}(i,1)$, for which $f_{4,7,8}(i,1)$ can be obtained from $f_4(i,2), f_7(i,1)$, and $f_8(i-1,2)$. The bounce back BC is typically used for static solid boundaries in the LBM model.

III. SIMULATION RESULTS

A. Simulation for silicon thin films

Under the framework of the proposed LBM model, we first calculate the thermal conductivity of the silicon thin films to validate the accuracy of this model. Consider an initially isothermal silicon thin film with thickness l and temperature T0. At time t = 0, the boundary temperature at y = 0 is suddenly changed to T1, and the boundary temperature at y = l is changed to T2, while the temperature at other locations is maintained at T = T0, as shown in Fig. 3(a).

The gray phonon properties of silicon used in this work are listed in Table I.

A representative temperature distribution inside an 820 nm thin film is shown in Figs. 3(b) and 3(c) by setting T1 = 299.5 K, T2 = 300.5 K, and T0 = 300 K. Figure 3(c) represents the temperature field predicted using the modified

TABLE I. Gray phonon properties of silicon.

Phonon relaxation time	$\tau = 6.53 \times 10^{-12}$ s
Phonon group velocity	$v = 6400$ m/s
Bulk thermal conductivity	$k = 148$ W/mK
Volumetric specific heat	$c_v = 1.66 \times 10^6$ J/m^{3}K
Phonon MFP	$\Lambda = 41.79 \times 10^{-9}$ m
Phonon frequency	$\omega = 8.18 \times 10^{13}$ rad/s
Density	$\rho = 2328$ kg/m^3

LBM model that incorporates the collision probability. The computed thermal conductivity in this case is approximately 131.9 W/m K, which is very close to the bulk thermal conductivity value of 148 W/m K. This suggests a near-diffusive thermal transport in the thin film.

In order to gain insight into how nondiffusive thermal transport affects the thin film thermal conductivity, we calculate the thermal conductivity of the silicon thin film for a range of thicknesses. When the film thickness is comparable with the phonon MFP, the long-MFP phonons travel ballistically through the film without undergoing massive scattering, which is inherently assumed by the Fourier diffusion law. As a result, the contribution to heat transport from those ballistic phonons is suppressed, which causes the thermal conductivity to decrease with the decrease in the film thickness. As shown in Fig. 3(d), the thermal conductivity depends strongly on the film thickness and can be two orders of magnitude lower than the bulk value for the accessible film thickness. Experimental results on cross-plane silicon thin film thermal conductivity has not yet been reported in literature. Instead, we compare the calculated thermal conductivity with the measured in-plane thermal conductivity in Fig. 3(d).[3,21,22] It is easy to find in the same film thickness situation that the in-plane thermal conductivity is slightly greater than that in the cross plane. This is because the phonon-boundary collision is more important in the cross-plane case than the in-plane case for the same film thickness. Thus, compared to the phonons in the cross-plane case, phonons in the in-plane case have a longer MFP. Therefore, the cross-plane thermal conductivity is slightly less than the experimental in-plane thermal conductivity.

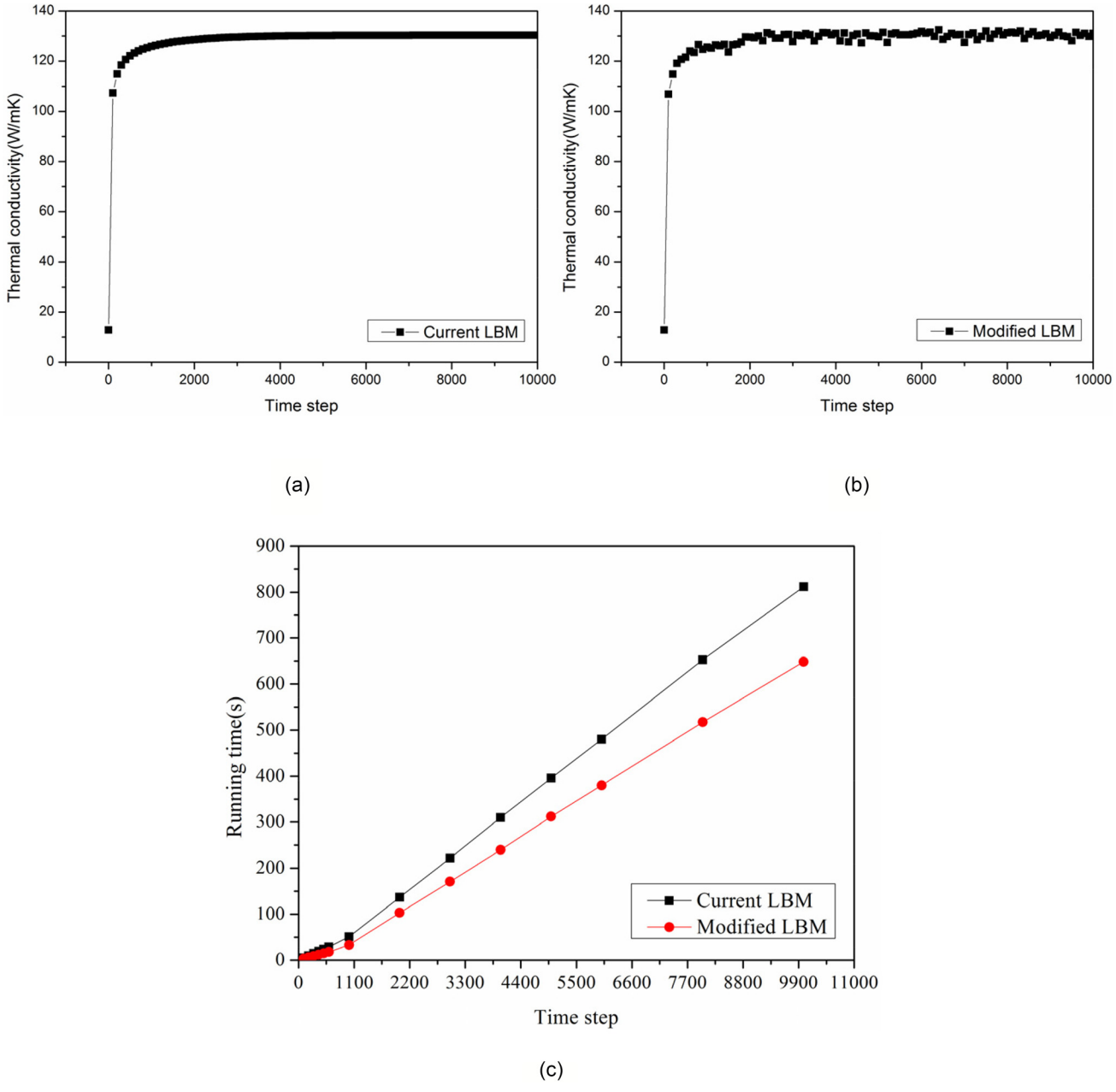

FIG. 4. Comparison of the computation efficiency of the current and modified LBMs. (a) The output value of the thermal conductivity with the time step using the current LBM. (b) The output value of the thermal conductivity with the time step using the modified LBM. (c) The running time of the current LBM and the modified LBM for a given time step.

One significant benefit of the newly developed LBM model is the improvement in the computational efficiency. Compared to the current LBM model, we find that the modified LBM model can substantially reduce the computational cost while maintaining the same accuracy. For example, Figs. 4(a) and 4(b) show the temporal evolution of the 820 nm thick film thermal conductivity simulated by the current LBM model and the modified LBM model, respectively. The value of the thermal conductivity is recorded for every 100 time steps. Although both models approach the final

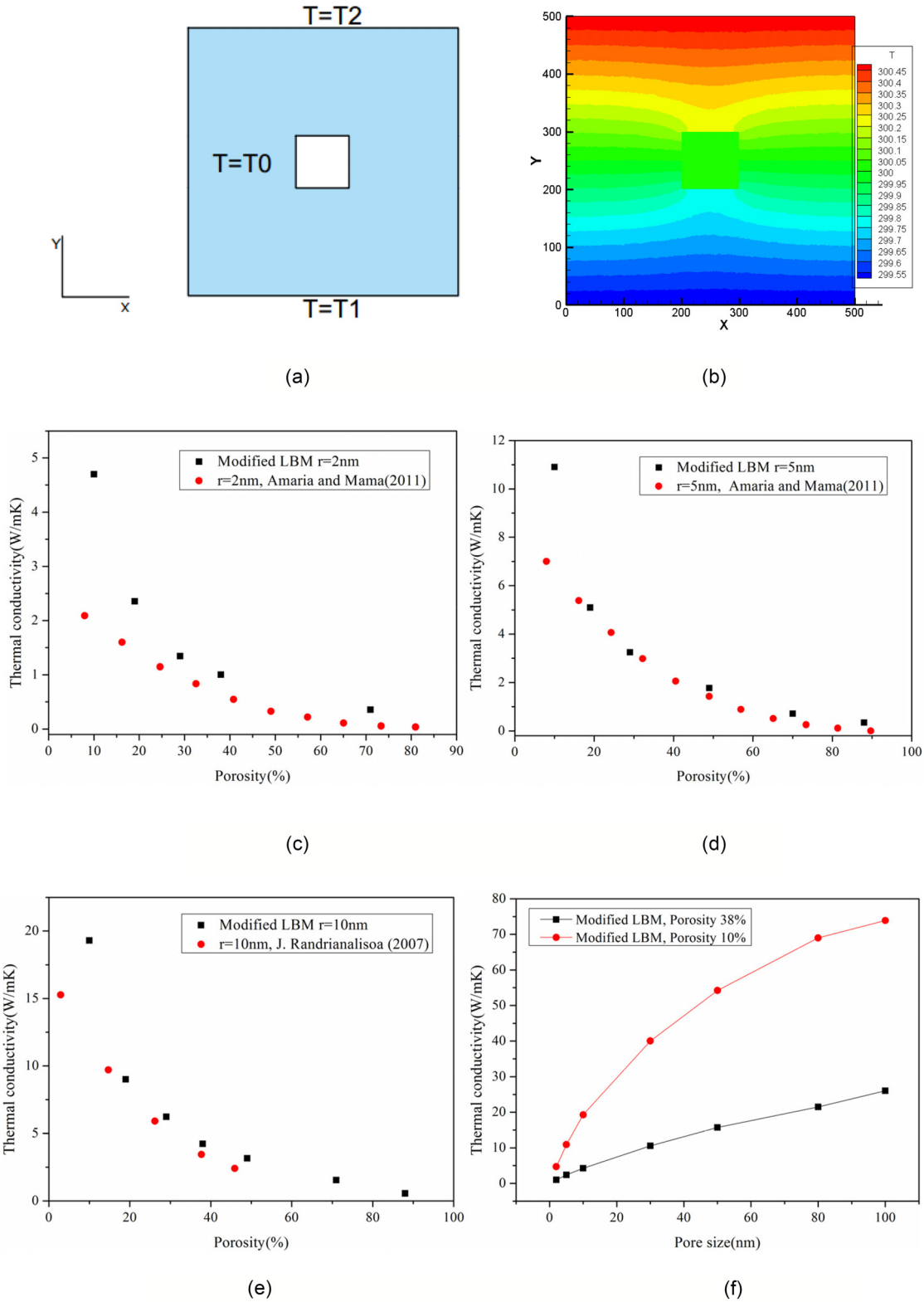

FIG. 5. D2Q9 lattice simulation for porous silicon. (a) Porous silicon simulation subject to constant temperature BCs. (b) Porous silicon temperature distribution using modified LBM. (c) Porosity dependence of thermal conductivity for r = 2 nm. (d) Porosity dependence of thermal conductivity for r = 5 nm. (e) Porosity dependence of thermal conductivity for r = 10 nm. (f) Pore size dependence of thermal conductivity at porosity of 38% and 10%.

thermal conductivity after approximately 3000 time steps, the running time of each time step in the modified model is significantly less than that of the current model, as shown in Fig. 4(c). It is clear that, accounting for all the time steps, the accumulative computational time is greatly reduced by the modified LBM model, particularly for complex structures. The computational efficiency of the modified LBM model originates from the introduction of the collision probability parameter. At each time step, as there is always a fraction of particles that have not experienced collision, their movements follow the rule of Eq. (6), which is easier for the computer to handle as compared to Eq. (7). Consequently, introducing a collision probability in the model can obviously improve the computational efficiency.

B. Simulation for porous silicon structures

We simulated thermal transport in porous silicon structures in this part. Owing to their unique low thermal conductivity and wide range of applications, porous silicon structures have been of research interest for a long time. A porous silicon film of thickness l, with a square pore of size $l1$, is simulated. In the initial time, we assume that the temperature of the porous structure maintained at T0. At time $t = 0$, the boundary temperature at $y = 0$ is suddenly changed to T1 and the boundary temperature at $y = l$ is changed to T2, while the interior domain still maintained at $T = T0$, as shown in Fig. 5(a). At the boundaries of the porous structure, we apply the bounce back BCs.

A representative steady state temperature distribution inside the porous structure predicted by the modified LBM model is shown in Fig. 5(b), where we set $l = 4100$ nm, $l1 = 820$ nm, $T1 = 299.5$ K, $T2 = 300.5$ K, and $T0 = 300$ K. For saving the simulation time and avoiding analogous work, only the modified LBM model is selected in this part simulation.

To gain insights into how different structure parameters affect the porous structure thermal conductivity, we perform simulations for a range of pore sizes and porosities and compare the results with previously reported experimental and numerical data,[23,24] as shown in Figs. 5(c)–5(f). As can be seen from Figs. 5(c) and 5(d), the calculated thermal conductivity for the pore sizes of 2 and 5 nm agree well with the experimental data in the high porosity range. However, a discrepancy between the computed thermal conductivity and measurement result occurs for lower values of porosity. This phenomenon is because when the porosity is large, the thermal conductivity is very small, so the relative errors between our simulation results and experiment results are smaller than the small porosity simulation. In Fig. 5(e), we compare the numerically determined thermal conductivity from this work and prior LBM studies for a 10 nm pore size structure. Figure 5(f) shows the pore-size-dependent thermal conductivity for two different porosities: 10% and 38%. It can be observed that a lower value of porosity corresponds to a greater value of thermal conductivity for the same pore size. This is because lower values of porosity lead to a bigger material size for a given pore size.

IV. CONCLUSION

In this study, we presented a modified LBM model incorporating a collision probability parameter to determine the occurrence of phonon scattering events at a lattice site. This treatment of phonon collision is analogous to the treatment of anharmonic scattering in the Monte Carlo simulation of nanoscale thermal transport. The developed algorithm, which exhibited significant computational improvement compared to the current LBM model, was applied to study length-dependent thermal transport in silicon thin films for a wide range of film thicknesses. We obtained a thickness-dependent thermal conductivity that was in good agreement with extant literature. The film thermal conductivity was found to decrease constantly with the decrease in thickness owing to an increasingly stronger ballistic transport effect. We also studied the thermal conductivity of porous silicon structures using the modified developed algorithm. The results for the porous silicon structures were in good agreement with the reported experimental and numerical data.

ACKNOWLEDGMENTS

This work was supported by the National Natural Science Foundation of China (Nos. 51776079 and 51736004) and the National Key Research and Development Program of China (No. 2017YFB0603501-3).

NOMENCLATURE

$\hbar$	reduced Planck's constant (J s)
k_b	Boltzmann's constant (J/K)
T_D	the Debye temperature (K)
D_ω	density of states ($1/m^3$)
f	probability distribution function
f^{eq}	equilibrium distribution function
$\vec{v}_g$	group velocity vector (m/s)
t	time (s)
q_n	thermal flux in direction n (W/m^2)
NX	lattice amounts in horizontal axis
ω	average phonon frequency (rad/s)
c_v	total specific heat (J/m^3 K)
τ	relaxation time of the particles (s)
α	lattice discrete direction
P	collision probability
Δt	time step (s)
$v_{g,\alpha}$	velocity in direction α (m/s)
x	position in space
T	temperature (K)
NY	lattice amounts in vertical axis

[1]D. G. Cahill, W. K. Ford, K. E. Goodson *et al.*, J. Appl. Phys. **93**(2), 793 (2003).
[2]A. D. McConnell and K. E. Goodson, Annu. Rev. Heat Transfer **14**(14), 129–168 (2005).
[3]H. Wang, Y. Xu, M. Shimono *et al.*, Mater. Trans. **48**(9), 2419 (2007).
[4]F. X. Alvarez, D. Jou, and A. Sellitto, Appl. Phys. Lett. **97**(3), 033103 (2010).
[5]G. Chen, *Nanoscale Energy Transport and Conversion: A Parallel Treatment of Electrons, Molecules, Phonons, and Photons* (Oxford University Press, USA, 2005).

[6]D. Jou, J. Casas-Vázquez, and G. Lebon, J. Non Equilibrium Thermodyn. **23**(3), 277 (1998).
[7]Z. M. Zhang, *Nano/Microscale Heat Transfer* (McGraw-Hill, New York, 2007).
[8]A. Nabovati, D. P. Sellan, and C. H. Amon, J. Comput. Phys. **230**(15), 5864 (2011).
[9]D. P. Sellan, J. E. Turney, A. J. H. McGaughey, and C. H. Amon, J. Appl. Phys. **108**(11), 113524 (2010).
[10]R. A. Escobar and C. H. Amon, J. Heat Transfer **130**(9), 092402 (2008).
[11]S. S. Ghai, W. T. Kim, R. A. Escobar, and C. H. Amon, J. Appl. Phys. **97**, 10P703 (2005).
[12]R. A. Escobar, S. S. Ghai, M. S. Jhon, and C. H. Amon, Int. J. Heat Mass Transfer **49**, 97 (2006).
[13]P. Heino, Comput. Math. Appl. **59**, 2351 (2010).
[14]A. Christensen and S. Graham, Numer. Heat Transfer, B **57**, 89 (2010).
[15]W. S. Jiaung and J. R. Ho, Phys. Rev. E **77**(6), 066710 (2008).
[16]J. E. Turney, A. J. H. McGaughey, and C. H. Amon, J. Appl. Phys. **107**, 024317 (2010).
[17]Q. Hao, G. Chen, and M.-S. Jeng, J. Appl. Phys. **106**(11), 114321 (2009).
[18]P. L. Bhatnagar, E. P. Gross, and M. Krook, Phys. Rev. **94**(3), 511 (1954).
[19]S. Succi, *The Lattice Boltzmann Equation: For Fluid Dynamics and Beyond* (Oxford University Press, New York, 2001).
[20]A. V. Savin, Y. A. Kosevich, and A. Cantarero, Phys. Rev. B **86**, 064305 (2012).
[21]Y. S. Ju and K. E. Goodson, Appl. Phys. Lett. **74**, 3005 (1999).
[22]W. Liu and M. Asheghi, Appl. Phys. Lett. **84**, 3819 (2004).
[23]A. Ould-Abbas, M. Bouchaour, and N. E. C. Sari, Open J. Phys. Chem. **2**, 17521 (2012).
[24]J. Randrianalisoa and D. Baillis, J. Phys.: Conf. Ser. **92**(1), 012081 (2007).